Journal of
Ceramic Science
and Technology

The Effect of the Glass Phase on the Modulus of Rupture of High-Alumina Refractories

W. Yuan[*], Q. Zhu, C. Deng, H. Zhu

The State Key Laboratory of Refractories and Metallurgy, Wuhan University of Science and Technology, Wuhan 430081, P.R. China

Abstract

Owing to their high refractoriness and slag resistance, high-alumina refractories are widely used in the lining of steelmaking furnaces, glass furnaces and cement rotary kilns in high-temperature industries. The impurities in the raw materials react to form the glass phase, which can melt into liquid at high temperatures. The modulus of rupture of refractories depends intensively on the content and composition of the glass phase. In this work, the cold and hot modulus of rupture for high-alumina bricks were investigated by means of fitting based on different theories. The effect of the glass phase on the modulus of rupture was analyzed by combining the phase composition, morphology of fracture surfaces and porosity for high-alumina refractories.

Keywords: Modulus of rupture, high-alumina refractories, glass phase

I. Introduction

High-alumina refractories are defined as those containing more than 45 % alumina (Al_2O_3) [1]. According to their alumina content, high-alumina bricks are subdivided into three categories as class A (45 – 65 %), B (65 – 75 %) and C (> 75 %) [2]. Because of their high refractoriness and slag resistance, high-alumina refractories are widely used in the lining of steelmaking furnaces, glass furnaces and cement rotary kilns. Various raw materials, including calcined bauxite, the sillimanite group of minerals (andalusite, sillimanite and kyanite), fused and sintered corundum as well as mullite, are used to produce high-alumina bricks [3, 4]. In order to replace expensive alumina, high-alumina products made from bauxite chamotte are manufactured on tonnage scale in Chinese refractory enterprises. For example, high-alumina bricks with 70 % alumina might contain a bauxite aggregate (about 90 % alumina) and various clay minerals containing less than 45 % Al_2O_3. This class of bricks is usually fired to relatively low temperatures to prevent excessive expansion, which leads to deviation in the final sizes.

The raw materials and their associated impurities impact on the quality and service life of any class of high-alumina bricks. For refractories, the phase equilibrium based on the overall composition is hardly reached. Generally, the fired high-alumina bricks consist of mullite and corundum, silica and glass phase [5]. The raw materials contain amounts of alkalis (Na_2O and K_2O), iron oxide (Fe_2O_3), and titania (TiO_2) [6]. The above-mentioned impurities react with alumina and silica to form glass phase, which forms the liquid phase at high temperatures.

Modulus of rupture at elevated temperatures is a criterion to evaluate the strength of refractories in service. The cold and hot modulus of rupture (CMOR and HMOR) of high-alumina refractories were studied based on comparison of the grain size of mullite and the retained strength after quench cycles [7, 8]. Stress-strain curves, elastic modulus and modulus of rupture of high-alumina bricks were investigated [9]. Regarding raw materials with the limited amounts of impurities, the quantity of glass phase in high-alumina ceramics has been determined as ranging from 10 to 15 % [10]. The presence of a considerable content of glass phase has a great influence on the evolution of phase, microstructure and mechanical properties [11 – 13]. Because the glass phase is unstable during service, it was found to be difficult to predict the mechanical properties of refractories at elevated temperatures, especially the correlation between the modulus of rupture and temperature, which was significant for the development of long-life refractories. However, further studies are required.

The aim of the present work is to evaluate the effect of the glass phase on the modulus of rupture of high-alumina refractories. For this purpose, the chemical and phase composition, porosity, cold and hot modulus of rupture of high-alumina refractories were characterized. In order to understand the interaction between the glass phase and corundum, thermodynamic calculations were performed. The fractal dimensions of fracture surface of high-alumina refractories were analyzed.

II. Experimental Procedure

One typical type of high-alumina bricks produced by a domestic enterprise was selected. The chemical compositions of the overall, crystalline and glass phase were measured by means of inductively coupled plasma atomic emission spectroscopy (ICP-AES, IRIS Advantage ER/S, Thermo Elemental, USA) following GB/T 6900 – 2006 and the acid leaching method reported in [14].

* Corresponding author: yuanwenjie@wust.edu.cn

High-alumina bricks were cut into several samples in the size of 25 mm × 25 mm × 150 mm. The surfaces of samples were polished. CMOR and HMOR at 1000 – 1400 °C for the bar samples were tested with a tester made by Luoyang Precondar Instruments Co. Ltd according to GB/T 3001 – 2007 and 3002 – 2004 standards. The average value of five samples was used to determine values for different temperatures. The apparent porosity of samples was evaluated with the Archimedes technique (GB/T 2997 – 2000). Closed porosity of samples was calculated based on the true density measured by using pycnometer (AccuPyc 1330, Micromeritics, USA).

The phase composition of the castables was analyzed by means of X-ray diffraction with CuKα radiation (XRD, Philips, X'pert Pro MPD, Netherlands). XRD results were quantitatively evaluated by means of the RIR method (MDI Jade 6.0, USA). The photos of whole fracture surfaces were taken with a digital camera. The fractal dimension of fracture surfaces was estimated with the slit island method. The photos were converted to grayscale images based on a certain threshold. The white-colored area in grayscale images was considered the "island". The area A and the perimeter P of each "island" were determined with Image-Pro Plus 6.0 software. The fractal dimension D was calculated based on a rectilinear slope of (D-1)/2 in the logP-logA scale curve [15].

The phase equilibrium calculations for the glass phase were performed with the FactSage software (version 6.2). The interactions between the glass phase and corundum were modeled from 1000 to 1400 °C with the addition of corundum (x) to the glass phase (1-x).

III. Results and Discussions

The chemical compositions of high-alumina bricks including overall, crystalline phase and glass phase are shown in Table 1. Mullite is the only stable intermediate phase with 71.6 wt% Al_2O_3 according to the Al_2O_3-SiO_2 diagram [16]. The equilibrium state was not reached particularly in the fired refractory. The Al_2O_3/SiO_2 ratio of 1.83 for the overall composition indicated that there was excess alumina in the bricks compared to the stoichiometric mullite. The amount of glass phase in high-alumina bricks was 13.03 wt%, which was close to the value for high-alumina refractories based on kaolin [17]. The impurities except Fe_2O_3 in the glass phase were somewhat higher than in the overall bricks. The lowest solidus line temperature in a six-component Al_2O_3-SiO_2-TiO_2-Fe_2O_3-CaO-MgO system was less than 1130 °C [18], which demonstrated that

the glass phase in the bricks would melt into liquid at high temperatures. Regarding the acid-insoluble residue as the crystalline phase, the major phases were considered to be corundum and mullite on account of high Al_2O_3/SiO_2 ratio of 2.65.
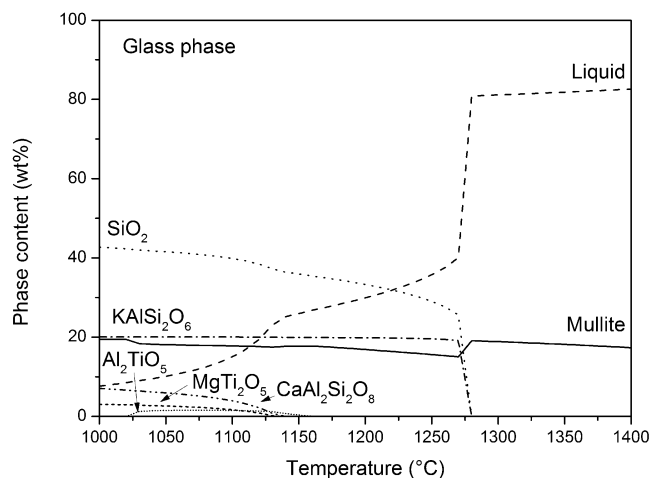

Fig. 1: Thermodynamic simulations of the glass phase obtained by means of chemical analysis.

The chemical composition of the glass phase presented in Table 1 was used as input values for the thermodynamic calculations to predict the phase composition at high temperatures, as shown in Fig. 1. Minor phases such as $CaAl_2Si_2O_8$, $MgTi_2O_5$ and Al_2TiO_5 only existed below 1200 °C. The content of liquid drastically increased above 1280 °C, meanwhile silica and leucite ($KAlSiO_4$) completely dissolved into the liquid. At 1400 °C, the equilibrium phases included 82.6 % liquid and 17.4 % mullite with regard to the glass composition. Similarly, it was reported that the fired porcelain comprised 10 – 25 % mullite and 65 – 80 % potassium aluminosilicate glass [19]. In compliance with the glass formation boundary concept [20], non-equilibrium conditions for the porcelain could be estimated based on leucite-mullite-silica phase diagram. Owing to the limitation of the solubility of alumina in the glass, excess alumina takes part in the mullite formation. For the glass composition obtained by chemical analysis, the composition of liquid phase shifted to the glass formation boundary with the temperature, which demonstrated that the liquid phase could be solidified as the glassy phase after cooling. In spite of the inhomogeneity for refractories, the above-mentioned analysis was of great value for evaluating the glass phase in refractories.

Table 1: Chemical composition of high-alumina bricks (overall, crystalline phase and glass phase) measured with the acid-etched method and ICP

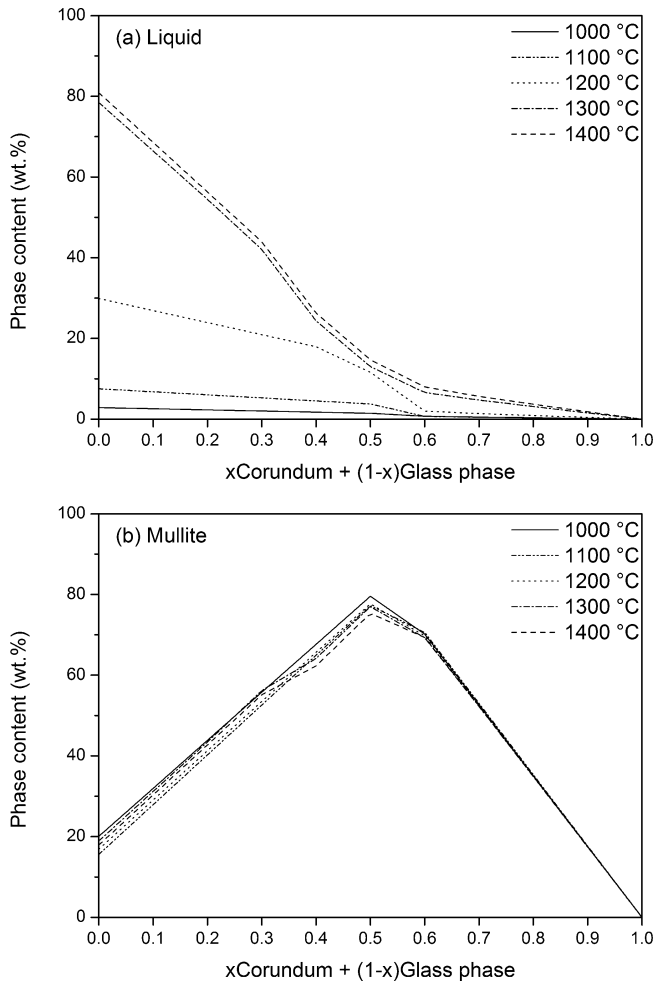|	Chemical composition (wt%)								Al_2O_3/ SiO_2	Mass fraction (wt%)
	SiO_2	Al_2O_3	Fe_2O_3	CaO	MgO	K_2O	Na_2O	TiO_2		
Overall	22.27	69.25	2.20	0.47	0.46	0.54	0.10	2.98	1.83	100
Crystalline phase	17.01	76.65	2.37	0.32	0.43	0.04	0.08	2.69	2.65	86.97
Glass phase	64.17	22.21	1.19	1.65	0.74	4.33	0.22	5.50	0.20	13.03

Fig. 2: Predicted phase content ((a) liquid and (b) mullite) on the interface between glass and corundum by means of thermodynamic simulations.

The transport and diffusion in the liquid were quicker at high temperatures. Therefore, the interaction between corundum and glass should be considered. The predicted equilibrium compositions (only selected liquid and mullite) on the interface of glass in contact with corundum are shown in Fig. 2. The left side (x = 0) and right side (x = 1) were regarded as the glass phase (taken from Table 1) and corundum respectively. It can be seen that the prominent reaction occurred at the interface of glass and corundum. Liquid gradually penetrated into the corundum side with the temperature (Fig. 2(a)). High amounts of mullite formed at the interface region, and the mullite content on the interface-near corundum side was almost independent of the temperature (Fig. 2(b)). For the localized composition, mullite was formed *in situ* at the expense of the liquid and corundum, which bonded with each other to obtain a mullitic binder matrix [21]. The variation of mullite and corundum content in high-alumina refractories after modulus of rupture tests at different temperatures was evaluated with the reference intensity ratio (RIR) method based on XRD patterns as seen in Fig. 3. The corundum content dropped off as the result of the increase of mullite content with the test temperatures, which differed from the trend presented in Fig. 2(b). Thus, the phase evolution for refractories was controlled by kinetic rather than thermodynamic factors. Owing to the sintering and pores fill-

ing with liquid, the total porosity as well as closed porosity of high-alumina refractories generally dropped with the test temperatures from Fig. 4, which was evident of the effect of glass phase on the densification [22].

The hot modulus of rupture for the refractory castables has been described using the models based on the Varshni and Adam-Gibbs theories for different temperatures [23]. In Varshni theory (VT) model, HMOR (σ) is given by the following formula:

$$\sigma = A - \frac{B}{\exp(C/T) - 1} \qquad (1)$$

where T is the thermodynamic temperature, A, B and C are parameters.

In the Adam-Gibbs (AG) theory, HMOR (σ) is assumed to be proportional to viscosity at high temperature. The equation can be written as:

$$\ln\sigma = A' + \frac{B'}{T\ln(T/C')} \qquad (2)$$

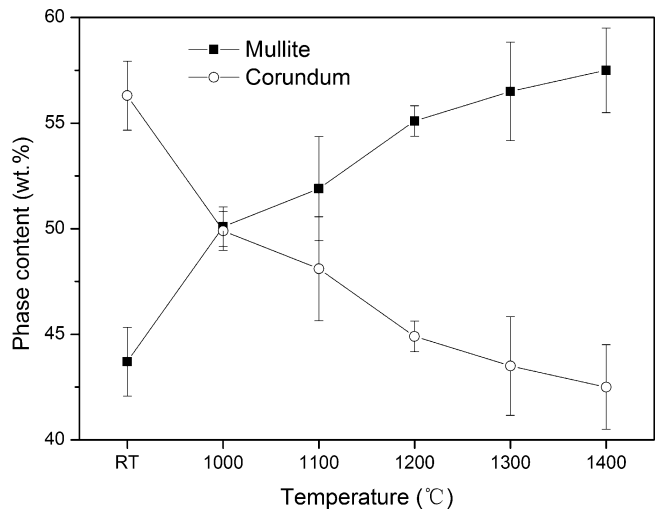where T is the thermodynamic temperature, A', B' and C' are parameters.

Fig. 3: The contents of mullite and corundum in high-alumina refractories after modulus of rupture tests at different temperatures.
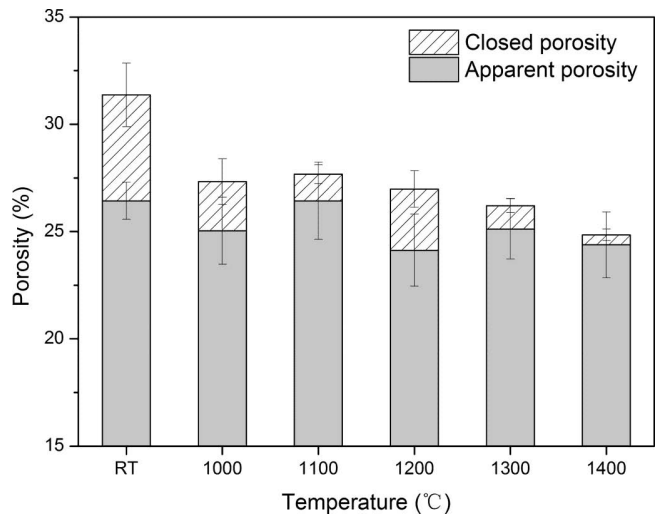

Fig. 4: The porosity of high-alumina refractories after modulus of rupture tests at different temperatures.

Fig. 5 illustrates the hot modulus of rupture values for high-alumina refractories, in which the lines indicate the calculated data. The mechanical behavior of high-alumina bricks at elevated temperatures may be divided into three stages: elastic, plastic and viscous flow stages[9]. HMOR values dropped with the increase in the test temperatures, which indicated that the contribution of the mullite formation and densification to the strength was limited. Changes of HMOR at different temperature ranges presented the distinct trends. For instance, the decline in the HMOR was 12.3 MPa from 1000 °C to 1250 °C, while it was 4.1 MPa from 1250 °C to 1400 °C corresponding to the viscous flow stage. However, the HMOR above 1250 °C fell to the level of less than 7 MPa, which was only 1/3 of the value at 1000 °C. The phenomenon could be attributable to the increase in liquid content above 1280 °C and bridging of liquid phases at high temperatures[24].
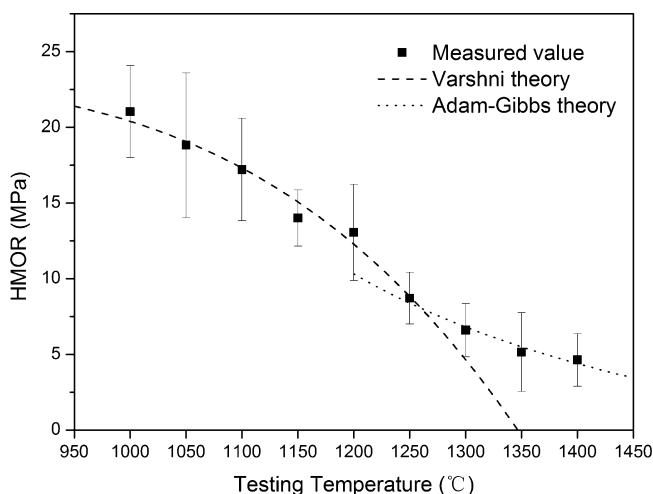

Fig. 5: Comparison of measured and predicted hot modulus of rupture (HMOR) values.

The temperature dependence of HMOR was fitted with the VT and AG models for the temperature below and above 1250 °C respectively. The fitted parameters are listed in Table 2. Considering the weakening of bonds in front of the crack tip[25], the temperature ($T_{0\,MPa}$) corresponding to zero strength based on VT model was 1346.7 °C, which was higher than that of castables (1279 – 1300 °C)[23]. High-alumina bricks were superior to cement-bonded castables with regard to this aspect. The transition of fracture mechanism as a result of the glass phase was shown at high temperatures. Owing to the viscous bridging in the following wake region, HMOR values would not reach zero at $T_{0\,MPa}$ in practice. HMOR at 1600 °C ($\sigma_{1600°C}$) calculated based on extrapolation according to measured data was little more than that of no-cement castables[23]. However, the degradation of high-alumina bricks depended on various factors including physical, chemical and mechanical. The impurities especially Fe_2O_3 and TiO_2 resulted in an increase of glass phase and a decrease of its viscosity at high temperatures, which could speed up creep of refractories[26]. Titanium-bearing slag with high alkali content severely attacked high-alumina bricks[27]. So this type of high-alumina bricks with high impurity level did not satisfy the

rigorous requirements for some specific applications such as hot blast stove and glass tank furnace. The glass phase was deduced as the key factor of service life for refractories at high temperatures.

Table 2: The fitted parameters of VT and AG model and the predicted values (the temperature at which HMOR equals zero, $T_{0\,MPa}$ and HMOR at 1600 °C, $\sigma_{1600°C}$).

VT model		AG model	
A (MPa)	23.52	A' (MPa)	-7.22
B (MPa)	38793.51	B' (MPa)	10000
C (MPa)	12000	C' (MPa)	1000
$T_{0\,MPa}$ (°C)	1346.7	$\sigma_{1600°C}$ (MPa)	1.29

Irregular fracture surfaces could be characterized by using the fractal dimension based on self-similarity[28]. The correlation between fractal dimension and mechanical properties depended on the microstructure and phase of the materials[29,30]. The comparison of fractal dimension and modulus of rupture indicated that variation of fracture behavior was not straightforward as shown in Fig. 6. Although HMOR at 1000 °C was higher than CMOR as the consequence of the reaction and sintering, the fractal dimension for high-alumina bricks was proportional to the flexural strength in the temperature regions of room temperature (RT)-1000 °C and 1050 °C – 1150 °C. On the contrary, the fractal dimension increased with the further decline of HMOR at the temperature above 1150 °C. It could be taken into account that pullout mechanism became more and more dominant for high-alumina bricks at high temperatures owing to the glass softening and liquid flow.
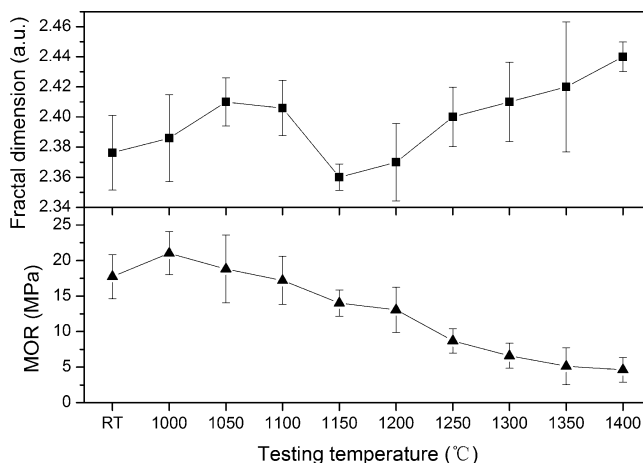

Fig. 6 : The variation of fractal dimension and modulus of rupture (MOR) for high-alumina refractories with the temperature.

IV. Conclusions

The glass phase has a significant influence on the hot modulus of rupture of high-alumina refractories. The porosity of high-alumina bricks after calcining at high temperatures decreased owing to the liquid phase sintering and the mullite formation. The modulus of rupture

of high-alumina refractories at 1000 °C was higher than that at room temperature. HMOR gradually decreased with the elevated temperature and fell off especially above 1250 °C because of the melting and viscous flow of the glass phase. The measured data of HMOR have been described by Varshni theory in the temperature range from 1000 °C to 1250 °C and by Adam-Gibbs theory above 1250 °C. Moreover, HMOR at higher temperatures could be predicted based on the latter model. Fracture surfaces in high-alumina refractories exhibit fractal characteristics over the range of the scales. The variation of HMOR with the temperature (above 1150 °C) is inversely proportional to the fractal dimension, which demonstrated that the degradation of refractories was accelerated by the glass phase.

Acknowledgments

References

1 Li, N., Gu, H.Z., Zhao, H.Z.: Refractories, Metallurgical Industry Press, Beijing, 2010.

2 Budnikov, P.P.: The technology of ceramics and refractories. The M.I.T. Press, Massachusetts, 1964.

3 Routschka, G.: Pocket manual refractory materials: Basics, structures, properties, Vulkan-Verlag GmbH, Essen, 2004.

4 Tripathi, H.S., Ghosh, A., Halder, M.K., Mukherjee, B., Maiti, H.S.: Microstructure and properties of sintered mullite developed from indian bauxite, *Bull. Mater. Sci.*, **35**, [4], 639 – 643, (2012).

5 Abou-Sekkina, M.M., Abo-El-Enein, S.A., Khalil, N.M., Shalma, O.A.: Phase composition of bauxite-based refractory castables, *Ceram. Int.*, **37**, [1], 411 – 418, (2011).

6 Maldhure, A.V., Tripathi, H.S., Ghosh, A., Das, S.K.: Mullite-corundum composites from bauxite: effect of chemical composition, *Trans. Indian Ceram. Soc.*, **73**, [1], 31 – 36, (2014).

7 Aksel, C.: The effect of mullite on the mechanical properties and thermal shock behaviour of alumina-mullite refractory materials, *Ceram. Int.*, **29**, [2], 183 – 188, (2003).

8 Andrews, A., Mothle, T.S., Olubambi, P.A.: Strength behaviour of alumina based refractories after thermal cycling, *J. Aust. Ceram. Soc.*, **49**, [2], 47 – 51, (2013).

9 Xu, E.X., Zhong, X.C.: Bending stress-strain relationship of high alumina bricks at elevated temperatures, (in Chinese), *Refract.*, **39**, [4], 266 – 269, (2005).

10 Kopeykin, V.A., Poluboyarinov, D.N.: Phase composition of high-alumina ceramics, *Refract.*, **1**, [11 – 12], 452 – 457, (1960).

11 Serry, M.A., El-Maghraby, M.S., Salama, S.Z.: Shaped aluminosilicate refractories from egyptian raw materials, *Am. Ceram. Soc. Bull.*, **85**, [9], 9201 – 9206, (2006).

12 Amutha, R.D., Gnanam, F.D.: Sol-gel mullite as the self-bonding material for refractory applications. *Ceram. Int.*, **26**, [4], 347 – 350, (2000).

13 Dehghani, K., Allaire, C.: Changes in hot modulus of rupture with the characteristics of aluminosilicate refractories. In: Proceedings of 44th annual conference of metallurgists of CIM, Calgary, Canada, 2005, 247 – 258.

14 Xu, J.P.: The measurement of glass phase content in mullite, (in Chinese), *Phys. Test. Chem. Anal. Part B: Chem. Anal.*, **43**, [7], 605 – 606, (2007).

15 Mecholsky, J.J., Passoja, D.E., Feinberg-Ringel, K.S.: Quantitative analysis of brittle fracture surfaces using fractal geometry, *J. Am. Ceram. Soc.*, **72**, [1], 60 – 65, (1989).

16 Klug, F.J., Prochazka, S., Doremus, R.H.: Alumina-silica phase diagram in the mullite region, *J. Am. Ceram. Soc.*, **70**, [10], 750 – 759, (1987).

17 Shmitt-Fogelevich, S.P.: Change in phase composition of high-alumina refractories, *Refract.*, **9**, [11 – 12], 789 – 796, (1968).

18 Sharapova, V.V., Sereda, B.P., Boguslavskii, D.Y., Malyshev, I.P., Troyan, V.D., Troshenkov, N.A.: Prospects of the use of aluminosilicate refractories for aluminum electrolyzers. part 3. the role of the glass phase formed in the operation of aluminum electrolyzers, *Refract. Ind. Ceram.*, **48**, [6], 395 – 396, (2007).

19 Iqbal, Y., Lee, W.E.: Fired porcelain microstructures revisited, *J. Am. Ceram. Soc.*, **82**, [12], 3584 – 3590, (1999).

20 Carty, W.M.: Observations on the glass phase composition in porcelains, *Ceram. Eng. Sci. Proc.*, **23**, [2], 79 – 94, (2002).

21 Baspinar, M.S., Kara, F.: Optimization of the corrosion behavior of mullite refractories against alkali vapor via $ZrSiO_4$ addition to the binder phase, *Ceram-Silikáty*, **53**, [4], 242 – 249, (2009).

22 Sacks, M.D., Pask, J.A.: Sintering of mullite-containing materials: 1, effect of composition, *J. Am. Ceram. Soc.*, **65**, [2], 65 – 70, (1982).

23 Hamacek, J., Machacek, J., Kutzendorfer, J., Korsa, B., Fiala, J.: On the high temperature bending strength of castables, *Ceram-Silikáty*, **56**, [3], 198 – 203, (2012).

24 Schnieder, J., Lynen, L., Traon, N., Tonnesen, T., Telle, R.: Crack formation and shape of fracture surface in tabular-alumina-based castables with addition of specific aggregates, *J. Ceram. Sci. Tech.*, **5**, [2], 131 – 136, (2014).

25 Bradt, R.C., Harmuth, H.: The fracture resistance of refractories, *Refract. Worldforum*, **3**, [4], 129 – 135, (2011).

26 Terzic, A., Pavlovic, L., Milutinovic-Nikolic, A.: Influence of the phase composition of refractory materials on creep, *Sci. Sinter.*, **38**, [3], 255 – 263, (2006).

27 Xu, G.T., Diao, R.S., Du, H.G., Sun, X.W.: Study on erosion process of vanadium-titanium bearing slag with high alkali content on blast furnace lining, (in Chinese), *Iron Steel Vanadium Titanium*, **25**, [2], 27 – 34, (2004).

28 Baran, G.R., Roques-Carmes, C., Wehbi, D., Degrange, M.: Fractal characteristics of fracture surfaces, *J. Am. Ceram. Soc.*, **75**, [10], 2687 – 2691, (1992).

29 Nagahama, H.: A fractal criterion for ductile and brittle fracture, *J. Appl. Phys.*, **75**, [6], 3220 – 3222, (1994).

30 Yuan, W.J., Zhu, Q.Y., Deng, C.J., Zhu, H.X.: Fractal analysis of fracture surfaces in refractories, *China's Refract.*, **23**, [1], 27 – 31, (2014).